

# Tumor Imaging with 2 $\sigma$ -Receptor Ligands, $^{18}\text{F}$ -FE-SA5845 and $^{11}\text{C}$ -SA4503: A Feasibility Study

Aren van Waarde, PhD<sup>1</sup>; Anne Rixt Buursma, MSc<sup>1</sup>; Geke A.P. Hospers, PhD<sup>2</sup>; Kazunori Kawamura, PhD<sup>3</sup>; Tadayuki Kobayashi, MSc<sup>4</sup>; Kenji Ishii, MD<sup>3</sup>; Keiichi Oda, PhD<sup>3</sup>; Kiichi Ishiwata, PhD<sup>3</sup>; Willem Vaalburg, PhD<sup>1</sup>; and Philip H. Elsinga, PhD<sup>1</sup>

<sup>1</sup>PET Center, Groningen University Hospital, Groningen, The Netherlands; <sup>2</sup>Department of Medical Oncology, Groningen University Hospital, Groningen, The Netherlands; <sup>3</sup>Tokyo Metropolitan Institute of Gerontology, Tokyo, Japan; and <sup>4</sup>M's Science, Kobe, Japan

Our objective was to study 2 radioligands for visualization of  $\sigma$ -receptors with PET. **Methods:** Two radioligands— $\sigma_1$ -selective  $^{11}\text{C}$ -1-(3,4-dimethoxyphenethyl)-4-(3-phenylpropyl)piperazine ( $^{11}\text{C}$ -SA4503) and nonsubtype-selective 1-(4-(2'- $^{18}\text{F}$ -fluoroethoxy-3-methoxyphenethyl)-4-(3-(4-fluorophenyl)propyl)piperazine ( $^{18}\text{F}$ -FE-SA5845)—were evaluated for tumor imaging. **Results:** Binding studies to rat glioma cells (C6) and human nonsmall cell lung cancer cells (N417) indicated interaction of  $^{18}\text{F}$ -FE-SA5845 with 2 sites and interaction of  $^{11}\text{C}$ -SA4503 with a single site. Specific binding of  $^{18}\text{F}$ -FE-SA5845 was  $93\% \pm 2\%$  and that of  $^{11}\text{C}$ -SA4503 was  $78\% \pm 6\%$  of the total cellular uptake of radioactivity. Uptake of the  $^{18}\text{F}$ -labeled ligand, but not that of the  $^{11}\text{C}$ -labeled ligand, appeared to be related to the growth phase of the cells. Biodistribution experiments in C6 tumor-bearing nude rats (Ham HSD RNU rnu) indicated tumor-to-plasma ratios of 13.3 for  $^{11}\text{C}$ -SA4503 and 8.0 for  $^{18}\text{F}$ -FE-SA5845 and tumor-to-muscle ratios of 5.0 for  $^{11}\text{C}$ -SA4503 and 4.9 for  $^{18}\text{F}$ -FE-SA5845, 60 min after injection, which were reduced to values ranging from 1.4 to 2.0 after pretreatment of animals with haloperidol (2  $\mu\text{mol}/\text{kg}$ ). Tumor uptake of  $^{18}\text{F}$ -FE-SA5845 showed a negative correlation with tumor size ( $P < 0.0001$ ), in contrast to that of  $^{11}\text{C}$ -SA4503, suggesting that tissue binding of the former ligand is related to cellular proliferation. A study with  $^{11}\text{C}$ -SA4503 in a human volunteer indicated high uptake in liver, kidney, and heart but relatively low background in thorax and lower abdomen. **Conclusion:** Both  $^{18}\text{F}$ -FE-SA5845 and  $^{11}\text{C}$ -SA4503 demonstrate specific binding to  $\sigma$ -receptors in vivo and may be useful for the detection of pulmonary and abdominal tumors. However, the  $^{18}\text{F}$ -labeled compound may be better for tumor staging than the  $^{11}\text{C}$ -labeled drug.

**Key Words:** tumor imaging; PET;  $\sigma$ -receptors; cellular proliferation; SA4503

J Nucl Med 2004; 45:1939–1945

The most widely used radiopharmaceutical in clinical oncology is  $^{18}\text{F}$ -FDG. Although the applications of  $^{18}\text{F}$ -FDG PET in tumor detection, staging, and therapy evaluation are

rapidly expanding,  $^{18}\text{F}$ -FDG uptake is not tumor specific. Various forms of inflammatory lesions also take up  $^{18}\text{F}$ -FDG and are a major cause of false-positive results. A decreased uptake of  $^{18}\text{F}$ -FDG is seen in hyperglycemic patients, which can cause false-negative scan data. Because of the urinary excretion of  $^{18}\text{F}$ -FDG, tumors in the lower abdomen (e.g., prostate tumors) are relatively poorly visualized. Thus, there is opportunity for the development of novel tumor imaging agents that may lack some of the disadvantages of  $^{18}\text{F}$ -FDG.

$\sigma$ -Receptors are unique proteins with a high affinity for neuroleptics such as haloperidol (1). They are strongly overexpressed in a large variety of human tumors—for example, glioma, neuroblastoma, melanoma, and breast cancer (2–4). The endogenous ligands for these sites have not yet been identified, although neuroactive steroids such as progesterone have a high affinity for  $\sigma$ -receptors (5,6).

Two subtypes of the  $\sigma$ -receptor have been discerned:  $\sigma_1$  and  $\sigma_2$ , based on their opposite enantioselectivity for benzomorphans and different molecular masses (7). The  $\sigma_2$ -receptor density of tumors is a biomarker of cellular proliferation (8–10). Activation of intracellular  $\sigma_2$ -receptors increases cytosolic  $\text{Ca}^{2+}$  and induces apoptosis via a caspase- and p53-independent mechanism (1,11,12). Therefore,  $\sigma$ -agonists may be effective antineoplastic agents and chemosensitizers (12–14).

A radioligand for visualization of  $\sigma$ -receptors with PET could be useful for (a) selective detection of primary tumors and their metastases, (b) noninvasive assessment of tumor proliferative status, and (c) measurement of the  $\sigma$ -receptor occupancy of novel and established antineoplastic drugs. We have evaluated 2 radioligands for these purposes.

SA4503 has a relatively high affinity for  $\sigma_1$ -receptors (50% inhibitory concentration [ $\text{IC}_{50}$ ], 17.4 nmol/L) but negligible affinity for the  $\sigma_2$ -subtype ( $\text{IC}_{50}$ , 1,784 nmol/L) and for 36 other neuroreceptors, ion channels, and second messenger systems (15). In contrast, its fluoroethyl analog, FE-SA5845, has a high affinity to both  $\sigma_1$ - and  $\sigma_2$ -receptors ( $\text{IC}_{50}$  values, 3.1 and 6.8 nmol/L, respectively) (16). The lipophilicity of both drugs is about optimal for entry of the central nervous system (log P values, +2.5 and +2.7, respectively) (16,17). In fact,  $^{11}\text{C}$ -SA4503 has been success-

Received Apr. 22, 2004; revision accepted July 14, 2004.

For correspondence or reprints contact: Philip H. Elsinga, PhD, PET Center, Groningen University Hospital, P.O. Box 30001, 9700RB Groningen, The Netherlands.

E-mail: p.h.elsinga@pet.azg.nl

fully used for PET studies of  $\sigma$ -receptors in cat, monkey, and human brain (18–21). Monkey studies with  $^{18}\text{F}$ -FE-SA5845 have also been performed (22).

Here, we report the results of in vitro and in vivo experiments in which  $^{18}\text{F}$ -FE-SA5845 and  $^{11}\text{C}$ -SA4503 were evaluated for tumor imaging.  $^{18}\text{F}$ -FE-SA5845 offers the advantages of a longer half-life of the radionuclide (109.8 min for  $^{18}\text{F}$  vs. 20.3 min for  $^{11}\text{C}$ ) and a high affinity to  $\sigma_2$ -receptors, which are the major subtype in tumor cells (3). In vivo assays of  $\sigma_2$ -receptor density may allow tumor staging (8–10). Since not only  $\sigma_2$ -receptors but also  $\sigma_1$ -receptors are present in most tumors (3) and the relationship between  $\sigma_1$ -receptor density and proliferative status is unknown,  $^{11}\text{C}$ -SA4503 could also be a successful imaging agent.

## MATERIALS AND METHODS

### Culture Media and Drugs

(+)-Pentazocine and (S)(-)-raclopride were purchased from Research Biochemicals International. Haloperidol was a product of Sigma. Unlabeled SA4503 was a gift from Santen Pharmaceutical Co. (S)-Ketamine (Ketanest) was purchased from Parke-Davis; Matrigel Basement Membrane Matrix was from BD Biosciences; and Dulbecco's Minimum Essential Medium (DMEM), fetal calf serum (FCS), and trypsin were from Invitrogen.

### Radioligands

$^{18}\text{F}$ -FE-SA5845 and  $^{11}\text{C}$ -SA4503 were prepared by reaction of  $^{18}\text{F}$ -fluoroethyl tosylate and  $^{11}\text{C}$ -methyl iodide, respectively, with the appropriate 4-*O*-demethyl compound, as described previously (16,17). The decay-corrected radiochemical yields of  $^{18}\text{F}$ -FE-SA5845 and  $^{11}\text{C}$ -SA4503 were 4%–7% and 9%–11%, respectively. Synthesis times were 80 and 45 min, respectively. The specific radioactivities of  $^{18}\text{F}$ -FE-SA5845 and  $^{11}\text{C}$ -SA4503 were >74 and >10 TBq/mmol at the time of injection. Radiochemical purities were >95%.

### Cell Culture

C6 rat glioma cells obtained from the American Type Culture Collection were cultured in monolayers in DMEM supplemented with 5% FCS in a humidified atmosphere of 5%  $\text{CO}_2$ /95% air at 37°C. Before each experiment, C6 cells were seeded in 12-well plates (Costar) with 1.5 mL of DMEM supplemented with 5% FCS per well. After 24 h at 37°C, monolayers had grown.

N417 human nonsmall cell lung cancer cells were grown in suspension in 25-cm<sup>2</sup> plastic flasks (Corning Co.) and cultured in DMEM with 10% FCS. After harvesting by centrifugation and resuspending in fresh medium, 1-mL samples of cell suspension in 15-mL test tubes were used for binding studies. All incubations were performed at 37°C in a shaking waterbath (Heidolph).

### Binding Studies: C6 Cells

Binding studies to C6 rat glioma cells were performed in monolayers grown at the bottom of 12-well plates. In competition studies, various concentrations of an unlabeled competitor (haloperidol, (+)-pentazocine, raclopride, or ketamine; range,  $10^{-12}$  to  $10^{-3}$  mol/L) were dispensed to the culture medium in the wells. At time zero, 2 MBq of radioligand in 50  $\mu\text{L}$  of saline were added to each well. At the end of incubation (60 min), the medium was

quickly removed and the monolayer was washed 3 times with phosphate-buffered saline (PBS). Cells were then treated with 0.25 mL of trypsin. When the cells had detached from the bottom of the well, 1 mL of DMEM was added to stop the proteolytic action. Cell clumps were removed by repeated (at least 10-fold) pipetting of the trypsin/DMEM mixture. Radioactivity in the cell suspension (1.2 mL) was assessed using a  $\gamma$ -counter (Compugamma 1282 CS; LKB-Wallac). A 50- $\mu\text{L}$  sample of the suspension was mixed with 50  $\mu\text{L}$  of trypan blue (0.4% solution in PBS) and used for cell counting. Cell numbers were manually determined, using a phase-contrast microscope (Zeiss), a Bürker bright-line chamber (depth, 0.1 mm; 0.0025-mm<sup>2</sup> squares), and a hand-tally counter. Nonspecific binding of the radioligand was defined as residual binding to the cells in the presence of an unlabeled competitor ( $5 \times 10^{-4}$  mol/L (+)-pentazocine, haloperidol, or unlabeled SA4503).

To study the influence of cell density on ligand binding, different numbers of C6 cells were seeded in various wells. After 1–4 d of growth in 12-well plates, cell densities ranged from 55,000 to 2,600,000 cells per well. Two megabecquerels of  $^{18}\text{F}$ -FE-SA5845 or  $^{11}\text{C}$ -SA4503 in 50  $\mu\text{L}$  of saline were then added. At the end of incubation (60 min), medium was quickly removed. Cells were washed, trypsinized, and counted as described.

### Binding Studies: N417 Cells

Binding studies to N417 cells were performed in test tubes containing a suspension of  $\sim 10^6$  cells/mL. In competition studies, various concentrations of an unlabeled competitor (haloperidol, (+)-pentazocine, ketamine, or SA4503; range,  $10^{-12}$  to  $10^{-3}$  mol/L) were dispensed to the culture medium in the tubes. At time zero, 2 MBq of radioligand in 50  $\mu\text{L}$  saline were added to each tube. At the end of incubation (60 min in most studies), the cells were harvested by centrifugation (10 s in a Hettich Micro 20 centrifuge at maximum speed, 14,000g). The cells were washed 3 times by resuspending them in PBS followed by repeated centrifugation. Removal of cell clumps, radioactivity, and cell counting were then performed as described.

### Biodistribution Experiments

The experiments were performed by licensed investigators in accordance with the Law on Animal Experiments of The Netherlands ("Wet op de Dierproeven" 1977 + Amendments 1996, "Dierproevenbesluit" 1985 + Amendments 1996). Female nude rats (HSD Ham RNU rnu; 150–200 g body weight) were obtained from Harlan. After 1 wk of acclimatization, C6 glioma cells ( $2.5 \times 10^6$ , in a 1:1 v/v mixture of Matrigel and DMEM containing 5% FCS) were subcutaneously injected into both flanks. Matrigel was included to avoid migration of tumor cells to other sites than the place of injection. Biodistribution studies were done after 9–10 d, when solid tumor nodules of 0.7- to 1.7-cm diameter had grown.

The rats were anesthetized using sodium pentobarbital (60 mg/kg intraperitoneal). Animals were kept under anesthesia for the rest of the experiment. The radiopharmaceutical (10 MBq  $^{18}\text{F}$ -FE-SA5845 or 20 MBq  $^{11}\text{C}$ -SA4503) was intravenously administered through a cannula inserted into a lateral tail vein. In blocking experiments, haloperidol (2  $\mu\text{mol/kg}$  in saline containing <10% ethanol) was administered 2 min before injection of the radioligand, through the same cannula, whereas control rats received saline only. The animals were sacrificed 60 min after radiotracer injection by extirpation of the heart (under general pentobarbital anesthesia). Blood was collected and normal tissues (brain, fat, bone, heart, intestines, kidney, liver, lung, skeletal muscle, pan-

creas, spleen, submandibular gland, and urinary bladder) were excised. Urine was collected and plasma plus a red cell fraction were obtained from blood centrifugation (5 min at 1,000g). The complete tumor was excised and carefully separated from muscle and skin. All samples were weighed, and the radioactivity was measured using the  $\gamma$ -counter, applying a decay correction. The results are expressed as dimensionless standardized uptake values (SUVs): cpm measured per gram of tissue/cpm injected per gram of body weight. Tumor-to-plasma and tumor-to-muscle concentration ratios of radioactivity were also calculated.

### Statistical Analysis

Statistical analysis was performed using the software package Statistix (NH Analytic Software). Differences between the various groups (control and haloperidol pretreated) were tested for statistical significance using the 2-sided Student *t* test for independent samples. *P* < 0.05 was considered significant.

### Human Study

A pilot study with  $^{11}\text{C}$ -SA4503 was performed on a volunteer. The study was approved by the Ethical Committee of the Tokyo Metropolitan Institute of Gerontology. A female subject (76 y old, 45.5 kg, 157.3 cm) participated, after written informed consent had been obtained. She had no clinical abnormality. The PET camera used was a SET-2400W type having an axial field of view of 20 cm (Shimadzu Co.) (23). Thirty-one minutes after intravenous injection of  $^{11}\text{C}$ -SA4503 (560 MBq/9.7 nmol) into the subject, a whole-body scan, spanning from head to legs, was performed in 2-dimensional mode (5 overlapping bed positions, 7-min emission time per position, with attenuation correction). Data were reconstructed using an ordered-subsets expectation maximization method (subsets, 16; iterations, 2). Pixel counts of the whole-body image were calibrated to activity concentration (Bq/mL).

## RESULTS

### Binding Studies in Tumor Cells

Initial in vitro studies showed rapid association of  $^{18}\text{F}$ -FE-SA5845 and  $^{11}\text{C}$ -SA4503 with tumor cells, equilibrium being reached after 20 min of incubation and remaining for >120 min at 37°C (values not shown). Therefore, an incubation time of 60 min was used in all subsequent experiments (24).

Competition studies using the  $\sigma_1$ -subtype-selective agonist (+)-pentazocine indicated binding of  $^{18}\text{F}$ -FE-SA5845 to 2 sites, both in the rodent and human cells. Biphasic competition was also observed for the nonsubtype-selective  $\sigma$ -ligand haloperidol (Table 1). The *N*-methyl-D-aspartate (NMDA) antagonist (*S*)-ketamine (which is often used for rodent anesthesia) and the dopamine  $\text{D}_2$ -receptor antagonist (*S*)-(-)-raclopride inhibited the binding of  $^{18}\text{F}$ -FE-SA5845 only at high concentrations ( $\text{IC}_{50}$  values in the  $10^{-5}$  to  $10^{-4}$  mol/L range; Table 1).

In contrast to  $^{18}\text{F}$ -FE-SA5845, (+)-pentazocine competition indicated binding of  $^{11}\text{C}$ -SA4503 to a single site, both in C6 and N417 cells. Monophasic inhibition of  $^{11}\text{C}$ -SA4503 binding was also observed in experiments using haloperidol and unlabeled SA4503 (Table 1). The NMDA antagonist (*S*)-ketamine inhibited the binding of  $^{11}\text{C}$ -SA4503 only at high concentrations ( $\text{IC}_{50}$  values in the  $10^{-5}$  to  $10^{-4}$  mol/L range; Table 1).

When  $^{18}\text{F}$ -FE-SA5845 was added to cells that either were actively growing or had become confluent, the equilibrium binding of the radioligand was found to be dependent on the growth phase. Rapidly growing cells showed a high uptake of  $^{18}\text{F}$ , but uptake in confluent cells was >5-fold reduced

**TABLE 1**  
Drug Interactions with Binding of  $\sigma$ -Receptor Ligands to Intact Tumor Cells

Competing drug	C6 cells (rat glioma)		N417 cells (human small cell lung carcinoma)	
	$\text{IC}_{50}$	<i>R</i>	$\text{IC}_{50}$	<i>R</i>
$^{18}\text{F}$ -FE-SA5845*				
(+)-Pentazocine ( $\sigma_1$ )	(0.3 nmol/L)/(13 $\mu\text{mol/L}$ )	0.987	(4.6 nmol/L)/(10 $\mu\text{mol/L}$ )	0.996
Haldol ( $\sigma_1$ , $\sigma_2$ , $\text{D}_2$ , $\text{D}_3$ )	(12 nmol/L)/(3.5 $\mu\text{mol/L}$ )	0.999	(0.1 $\mu\text{mol/L}$ )/(6.5 $\mu\text{mol/L}$ )	0.996
Raclopride ( $\text{D}_2$ )	200 $\mu\text{mol/L}$	0.991	27 $\mu\text{mol/L}$	0.995
( <i>S</i> )-Ketamine (NMDA)	ND	ND	52 $\mu\text{mol/L}$	0.998
$^{11}\text{C}$ -SA4503†				
(+)-Pentazocine ( $\sigma_1$ )	2.4 $\mu\text{mol/L}$	0.957	8.6 $\mu\text{mol/L}$	0.982
Haldol ( $\sigma_1$ , $\sigma_2$ , $\text{D}_2$ , $\text{D}_3$ )	0.1 $\mu\text{mol/L}$	0.997	0.3 $\mu\text{mol/L}$	0.994
SA4503 ( $\sigma_1$ )	0.2 $\mu\text{mol/L}$	0.998	ND	ND
( <i>S</i> )-Ketamine (NMDA)	22 $\mu\text{mol/L}$	0.998	45 $\mu\text{mol/L}$	0.998

\*Specific (haloperidol and (+)-pentazocine sensitive) binding of tracer as fraction of total uptake:  $93.2\% \pm 2.2\%$ .

†Specific (pentazocine, haloperidol, and SA4503 sensitive) binding of tracer as fraction of total uptake:  $78.3\% \pm 6.0\%$ .

*R* = correlation coefficient of curve fit; ND = not determined.

**FIGURE 1.** Relationship between growth stage (number of C6 cells per well) and cellular uptake of  $^{18}\text{F}$ -FE-SA5845 (A) and  $^{11}\text{C}$ -SA4503 (B). Ordinate indicates total bound radioactivity within cells. Dashed line is an exponential curve fit.

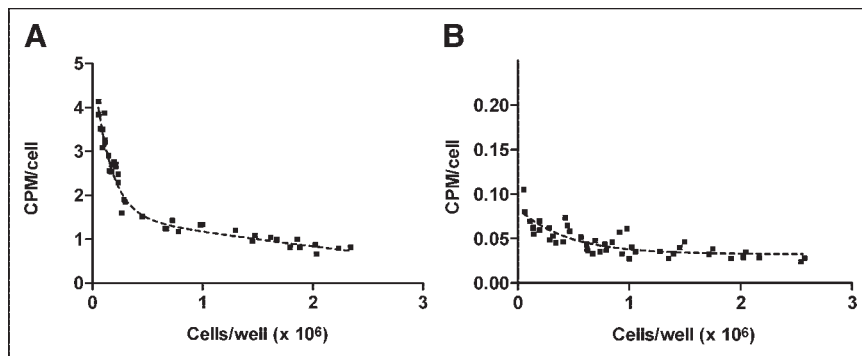


(Fig. 1). Different results were obtained with  $^{11}\text{C}$ -SA4503. Uptake of this tracer in confluent cells was only slightly ( $\sim 2$ -fold) reduced compared with that of actively growing cells (Fig. 1).

#### Biodistribution of $^{18}\text{F}$ -FE-SA5845

After injection of  $^{18}\text{F}$ -FE-SA5845 in tumor-bearing rats, the highest uptake of radioactivity was observed in liver, followed by kidney, pancreas, and lung. Submandibular gland, intestines, spleen, urinary bladder, brain, and C6 tumor showed moderate tracer uptake, whereas low levels

of radioactivity were found in heart, adipose tissue, bone, muscle, plasma, and red blood cells (Table 2).

Pretreatment of animals with haloperidol ( $2 \mu\text{mol/kg}$ ) caused a strong reduction of tissue uptake in brain, intestines, kidney, liver, and C6 tumors, whereas radioactivity in plasma and blood cells was increased. Radioactivity in spleen and submandibular gland seemed also to be decreased by haloperidol, but statistical significance ( $P < 0.05$ ) was not reached in these organs because of a relatively high interindividual variation. Control animals showed tumor-to-plasma and tumor-to-muscle ratios of 8.0 and 4.9, respectively, at 60 min after injection. These were reduced to low values (1.4–1.5) in pretreated rats (Table 2).

**TABLE 2**

Biodistribution of  $^{18}\text{F}$ -FE-SA5845 in Tumor-Bearing Rats 60 Minutes After Injection

Tissue	Control ( $n = 5$ )	Haloperidol ( $n = 5$ )	$P$
Cerebellum	$1.41 \pm 0.23$	$0.43 \pm 0.12$	$<0.0001$
Cerebral cortex	$1.26 \pm 0.31$	$0.45 \pm 0.16$	0.0005
Rest brain	$1.42 \pm 0.28$	$0.41 \pm 0.13$	0.0001
Adipose tissue	$0.46 \pm 0.18$	$0.45 \pm 0.26$	NS
Bladder	$1.61 \pm 0.94$	$0.95 \pm 0.45$	NS
Bone	$0.42 \pm 0.14$	$0.39 \pm 0.13$	NS
Heart	$0.47 \pm 0.16$	$0.66 \pm 0.25$	NS
Large intestine	$1.76 \pm 0.18$	$0.84 \pm 0.30$	0.0002
Small intestine	$2.35 \pm 0.44$	$1.13 \pm 0.35$	0.0006
Kidney	$4.95 \pm 0.84$	$1.77 \pm 0.58$	$<0.0001$
Liver	$9.28 \pm 1.50$	$5.58 \pm 2.24$	$<0.01$
Lung	$2.93 \pm 0.83$	$2.50 \pm 1.09$	NS
Muscle	$0.20 \pm 0.07$	$0.25 \pm 0.10$	NS
Pancreas	$4.23 \pm 0.85$	$4.39 \pm 2.69$	NS
Plasma	$0.12 \pm 0.03$	$0.23 \pm 0.05$	$<0.001$
Red blood cells	$0.08 \pm 0.01$	$0.16 \pm 0.05$	$<0.05$
Spleen	$2.05 \pm 0.46$	$1.43 \pm 0.53$	0.08
Submandibular	$2.33 \pm 0.85$	$1.31 \pm 0.73$	0.06
C6 tumor*	$0.92 \pm 0.39$	$0.37 \pm 0.18$	0.0005
Urine	$9.71 \pm 6.54$	$9.45 \pm 3.88$	NS
Tumor/plasma*	$8.0 \pm 3.2$	$1.4 \pm 0.9$	$<0.0001$
Tumor/muscle*	$4.9 \pm 2.8$	$1.5 \pm 0.9$	0.001

\*Twice as much data (2  $n$ ) since each rat had 2 tumors.

NS = not significant.

SUVs (and dimensionless ratios) are listed (mean  $\pm$  SD).

#### Biodistribution of $^{11}\text{C}$ -SA4503

The  $\sigma_1$ -subtype-selective radioligand  $^{11}\text{C}$ -SA4503 showed a biodistribution similar to that of nonsubtype-selective  $^{18}\text{F}$ -FE-SA5845. The highest uptake of radioactivity was observed in liver, followed by pancreas, small intestine, and kidney. Moderate tracer uptake was found in spleen, submandibular gland, large intestine, lung, urinary bladder, and the C6 tumor. Low uptake of  $^{11}\text{C}$  was observed in heart, bone, adipose tissue, muscle, plasma, and red blood cells (Table 3). Uptake of  $^{11}\text{C}$  in C6 tumors after injection of  $^{11}\text{C}$ -SA4503 tended to be lower than the uptake of  $^{18}\text{F}$  after administration of  $^{18}\text{F}$ -FE-SA5845 (SUV values in Table 2 compared with those in Table 3).

Pretreatment of animals with haloperidol ( $2 \mu\text{mol/kg}$ ) suppressed the uptake of  $^{11}\text{C}$ -SA4503 in target tissues. A reduction of tissue radioactivity was observed in brain, intestines, kidney, liver, and C6 tumors, whereas radioactivity in plasma, red blood cells, and myocardium was increased. However, radioactivity levels in spleen and submandibular gland were not reduced after haloperidol pretreatment.

Although tumor SUVs of  $^{11}\text{C}$ -SA4503 appeared to be lower than those of  $^{18}\text{F}$ -FE-SA5845, similar target-to-non-target ratios were measured for the 2 tracers. Control animals showed tumor-to-plasma ratios of 13.3 and tumor-to-muscle ratios of 5.0, 60 min after injection of  $^{11}\text{C}$ -SA4503.

**TABLE 3**  
Biodistribution of  $^{11}\text{C}$ -SA4503 in Tumor-Bearing Rats  
60 Minutes After Injection

Tissue	Control (n = 5)	Haloperidol (n = 3)	P
Cerebellum	1.06 ± 0.38	0.58 ± 0.05	<0.05
Cerebral cortex	1.24 ± 0.47	0.45 ± 0.01	<0.02
Rest brain	1.27 ± 0.40	0.48 ± 0.03	0.01
Adipose tissue	0.21 ± 0.07	0.68 ± 0.33	NS
Bladder	1.01 ± 0.69	0.87 ± 0.38	NS
Bone	0.27 ± 0.19	0.24 ± 0.14	NS
Heart	0.30 ± 0.09	0.69 ± 0.16	<0.005
Large intestine	1.59 ± 0.24	0.70 ± 0.16	<0.002
Small intestine	2.92 ± 0.91	0.89 ± 0.29	0.01
Kidney	2.89 ± 0.24	1.39 ± 0.07	0.0001
Liver	11.61 ± 2.28	4.81 ± 1.25	<0.005
Lung	1.55 ± 0.30	1.60 ± 0.24	NS
Muscle	0.19 ± 0.11	0.22 ± 0.02	NS
Pancreas	5.04 ± 4.39	3.40 ± 1.26	NS
Plasma	0.06 ± 0.02	0.24 ± 0.04	0.0001
Red blood cells	0.06 ± 0.03	0.13 ± 0.01	0.01
Spleen	2.43 ± 0.71	3.32 ± 0.42	NS
Submandibular	2.36 ± 0.77	3.78 ± 0.14	NS
C6 tumor*	0.65 ± 0.15	0.43 ± 0.15	<0.05
Urine	4.02 ± 2.86	7.29 ± 2.80	NS
Tumor/plasma*	13.3 ± 3.1	1.9 ± 0.9	<0.0001
Tumor/muscle*	5.0 ± 2.5	2.0 ± 0.7	<0.05

\*Twice as much data (2 n) since each rat had 2 tumors.  
NS = not significant.  
SUVs (and dimensionless ratios) are listed (mean ± SD).

These were reduced to low values (1.9–2.0) in pretreated rats (Table 3).

#### Size-Dependent Tracer Uptake

When tracer binding in individual tumors was plotted against tumor mass, the uptake of  $^{18}\text{F}$ -FE-SA5845 was found to be negatively correlated with tumor size (slope,  $-0.85 \pm 0.10$ ;  $r = 0.95$ ,  $P < 0.0001$ ; Fig. 2). Different results were observed for the in vivo uptake of  $^{11}\text{C}$ -SA4503. The uptake of this tracer did not show a significant relationship with tumor size (slope,  $-0.04 \pm 0.12$ ;  $r = 0.14$ ,  $P =$  not significant; Fig. 2).

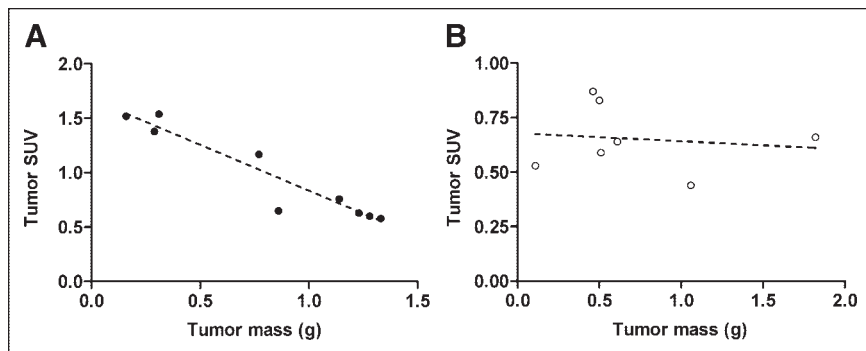


**FIGURE 2.** Relationship between tumor mass (in vivo C6 tumors grown in nude rats) and tumor uptake of  $^{18}\text{F}$ -FE-SA5845 (A) and  $^{11}\text{C}$ -SA4503 (B). Solid and open symbols are data points of individual tumors; dashed line is result of a linear regression analysis.

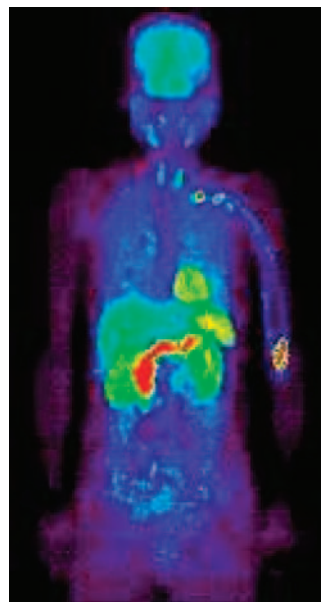


**FIGURE 3.** Whole-body scan of human volunteer, made 31–66 min after injection of  $^{11}\text{C}$ -SA4503.

#### Human Study

The human pilot study with  $^{11}\text{C}$ -SA4503 in a single volunteer (Fig. 3) indicated high uptake of the tracer in brain, heart, liver and kidneys, but a relatively low background of radioactivity in the thorax, extremities, and lower abdomen.

#### DISCUSSION

This study confirms that the nonsubtype-selective ligand  $^{18}\text{F}$ -FE-SA5845 binds to 2 sites and the  $\sigma_1$ -subtype-selective ligand  $^{11}\text{C}$ -SA4503 binds to a single site in intact tumor cells (Table 1). Probably, the 2 binding sites of  $^{18}\text{F}$ -FE-SA5845 are  $\sigma_1$ - and  $\sigma_2$ -receptors. In vitro competition experiments with the established  $\sigma_1$ -receptor agonists (+)-pentazocine and SA4503, or the  $\sigma$ -receptor antagonist haloperidol, indicated that the specific binding of  $^{18}\text{F}$ -FE-SA5845 was  $93\% \pm 2\%$  and of  $^{11}\text{C}$ -SA4503 was  $78\% \pm 6\%$  of the total cellular uptake of radioactivity, both in rodent and human cells (Table 1). Thus, the in vitro experiments suggest better signal-to-noise ratios for  $^{18}\text{F}$ -FE-SA5845 than for  $^{11}\text{C}$ -SA4503.  $^{18}\text{F}$ -FE-SA5845 and  $^{11}\text{C}$ -

SA4503 do not bind to dopamine D<sub>2</sub>-receptors or NMDA receptors on intact tumor cells, since the D<sub>2</sub>/D<sub>3</sub>-receptor antagonist raclopride and the NMDA antagonist (*S*)-ketamine inhibited the binding only at high concentrations (10<sup>-5</sup> to 10<sup>-3</sup> mol/L range).

Experiments in which the effect of the growth phase on the cellular uptake of the  $\sigma$ -ligands was examined indicated a marked decline in the uptake of <sup>18</sup>F-FE-SA5845, but a less marked decline in <sup>11</sup>C-SA4503 uptake, in confluent cells (Fig. 1). <sup>11</sup>C-SA4503 is selective for the  $\sigma_1$ -subtype, whereas <sup>18</sup>F-FE-SA5845 binds equally well to  $\sigma_1$ - and  $\sigma_2$ -receptors. Figure 1 is therefore in accordance with reports in the literature which suggest that the density of  $\sigma_2$ -receptors is related to the proliferative status of tumor cells (8–10). Using another cell line (66 cells rather than C6 cells), Mach et al. have shown that the  $\sigma_2$ -receptor density is >10-fold reduced in quiescent cells (8).

In biodistribution experiments (Tables 2 and 3), both <sup>18</sup>F-FE-SA5845 and <sup>11</sup>C-SA4503 showed specific (i.e., haloperidol sensitive) binding in C6 tumors and also in other target organs, such as brain, intestines, kidney, and liver. The high and haloperidol-sensitive uptake of <sup>18</sup>F-FE-SA5845 and <sup>11</sup>C-SA4503 in liver, kidney, and intestines is consistent with the reported high levels of  $\sigma_1$ -receptor messenger RNA (25,26) and high densities of  $\sigma_1$ - and  $\sigma_2$ -receptors in these excretory organs (27–30). Although both  $\sigma_1$ - and  $\sigma_2$ -receptors have been reported to be expressed on splenocytes (31,32), only <sup>18</sup>F-FE-SA5845 showed some specific binding in rat spleen (Table 2). Apparently, the  $\sigma_1$ -subtype-specific radioligand <sup>11</sup>C-SA4503 shows high nonspecific and little specific binding in rat spleen *in vivo*.

The biodistribution experiments indicated tumor-to-plasma ratios of 13.3 for <sup>11</sup>C-SA4503 and 8.0 for <sup>18</sup>F-FE-SA5845 and tumor-to-muscle ratios of 5.0 for <sup>11</sup>C-SA4503 and 4.9 for <sup>18</sup>F-FE-SA5845, 60 min after injection, which were reduced to values ranging from 1.4 to 2.0 after pretreatment of animals with haloperidol (Tables 2 and 3). These tumor-to-plasma ratios are higher than or equal to those of the radiopharmaceuticals <sup>18</sup>F-FDG and 3'-deoxy-3'-<sup>18</sup>F-fluorothymidine (<sup>18</sup>F-FLT), which were studied previously in the same *in vivo* tumor model (6.1 and 3.8, respectively) (33). The observed tumor-to-muscle ratios of the  $\sigma$ -ligands are also higher than those of <sup>18</sup>F-FLT (3.8  $\pm$  1.4) but lower than those of <sup>18</sup>F-FDG (13.2  $\pm$  3.0) (33).

Tumor uptake of the <sup>18</sup>F-labeled ligand tended to be higher than that of the <sup>11</sup>C-labeled agonist (SUV, 0.92  $\pm$  0.39 vs. 0.65  $\pm$  0.16, respectively; Tables 2 and 3). This trend is probably due to the fact that <sup>18</sup>F-FE-SA5845 binds to both  $\sigma_1$ - and  $\sigma_2$ -receptors (16), whereas <sup>11</sup>C-SA4503 interacts with  $\sigma_1$ -receptors only (15).

Another difference between the 2 radiotracers was observed when the SUV in individual tumors was plotted against tumor mass (Fig. 2). The SUV of <sup>18</sup>F-FE-SA5845 was negatively correlated with tumor size ( $P < 0.0001$ ), in contrast to tissue uptake of <sup>11</sup>C-SA4503. All tumors in these experiments showed only small areas of necrosis, amount-

ing to <10% of the total tumor volume. Thus, the decline in the SUV of <sup>18</sup>F-FE-SA5845 with increasing tumor size was not related to necrosis. Perfusion changes with increasing tumor size should have affected the uptake of both radioligands equally, since they have similar lipophilicities and the range of tumor sizes was similar in both cases (Fig. 2). Although no data on growth rate are available, the most likely explanation for the different behavior of the 2 ligands is that only the binding of <sup>18</sup>F-FE-SA5845 is related to cellular proliferation.

The human pilot study with <sup>11</sup>C-SA4503 indicated a relatively low background level of radioactivity in the extremities, thorax, and lower abdomen. Thus, <sup>11</sup>C-SA4503 may be useful for the detection of sarcomas, lung tumors and abdominal tumors, using PET.

## CONCLUSION

<sup>18</sup>F-FE-SA5845 and <sup>11</sup>C-SA4503 demonstrate specific binding to  $\sigma$ -receptors, both *in vitro* and *in vivo*. The observed target-to-nontarget ratios suggest that these radioligands may be suitable for tumor detection and for assessment of the  $\sigma$ -receptor occupancy of novel therapeutic drugs. The uptake of <sup>18</sup>F-FE-SA5845 was reduced in large tumors and quiescent cells, in contrast to the binding of <sup>11</sup>C-SA4503. Hence, <sup>18</sup>F-FE-SA5845 may be preferred over <sup>11</sup>C-SA4503 for tumor staging.

## ACKNOWLEDGMENTS

This work was partially supported by a Grant-in-Aid for Scientific Research (B) no. 13557077 from the Ministry of Education, Culture, Sports, Science and Technology, Japan.

## REFERENCES

1. Bowen WD. Sigma receptors: recent advances and new clinical potentials. *Pharm Acta Helv.* 2000;74:211–218.
2. Bem WT, Thomas GE, Mamone JY, et al. Overexpression of sigma receptors in nonneural human tumors. *Cancer Res.* 1991;51:6558–6562.
3. Vilner BJ, John CS, Bowen WD. Sigma-1 and sigma-2 receptors are expressed in a wide variety of human and rodent tumor cell lines. *Cancer Res.* 1995;55:408–413.
4. John CS, Bowen WD, Varma VM, McAfee JG, Moody TW. Sigma receptors are expressed in human non-small cell lung carcinoma. *Life Sci.* 1995;56:2385–2392.
5. Maurice T, Phan VL, Urani A, Kamei H, Noda Y, Nabeshima T. Neuroactive neurosteroids as endogenous effectors for the sigma1 receptor: pharmacological evidence and therapeutic opportunities. *Jpn J Pharmacol.* 1999;81:125–155.
6. Ueda H, Yoshida A, Tokuyama S, et al. Neurosteroids stimulate G protein-coupled sigma receptors in mouse brain synaptic membrane. *Neurosci Res.* 2001;41:33–40.
7. Quirion R, Bowen WD, Itzhak Y, et al. A proposal for the classification of sigma binding sites. *Trends Pharmacol Sci.* 1992;13:85–86.
8. Mach RH, Smith CR, al Nabulsi I, Whirrett BR, Childers SR, Wheeler KT. Sigma 2 receptors as potential biomarkers of proliferation in breast cancer. *Cancer Res.* 1997;57:156–161.
9. Wheeler KT, Wang LM, Wallen CA, et al. Sigma-2 receptors as a biomarker of proliferation in solid tumours. *Br J Cancer.* 2000;82:1223–1232.
10. al Nabulsi I, Mach RH, Wang LM, et al. Effect of ploidy, recruitment, environmental factors, and tamoxifen treatment on the expression of sigma-2 receptors in proliferating and quiescent tumour cells. *Br J Cancer.* 1999;81:925–933.
11. Brent PJ, Pang G, Little G, Dosen PJ, Van Helden DF. The sigma receptor ligand, reduced haloperidol, induces apoptosis and increases intracellular-free calcium levels [Ca<sup>2+</sup>]<sub>i</sub> in colon and mammary adenocarcinoma cells. *Biochem Biophys Res Commun.* 1996;219:219–226.

12. Crawford KW, Bowen WD. Sigma-2 receptor agonists activate a novel apoptotic pathway and potentiate antineoplastic drugs in breast tumor cell lines. *Cancer Res.* 2002;62:313–322.
13. Brent PJ, Pang GT. Sigma binding site ligands inhibit cell proliferation in mammary and colon carcinoma cell lines and melanoma cells in culture. *Eur J Pharmacol.* 1995;278:151–160.
14. Barbieri F, Sparatore A, Alama A, Novelli F, Bruzzo C, Sparatore F. Novel sigma binding site ligands as inhibitors of cell proliferation in breast cancer. *Oncol Res.* 2003;13:455–461.
15. Matsuno K, Nakazawa M, Okamoto K, Kawashima Y, Mita S. Binding properties of SA4503, a novel and selective sigma 1 receptor agonist. *Eur J Pharmacol.* 1996;306:271–279.
16. Kawamura K, Elsinga PH, Kobayashi T, et al. Synthesis and evaluation of <sup>11</sup>C- and <sup>18</sup>F-labeled 1-[2-(4-alkoxy-3-methoxyphenyl)ethyl]-4-(3-phenylpropyl)piperazines as sigma receptor ligands for positron emission tomography studies. *Nucl Med Biol.* 2003;30:273–284.
17. Kawamura K, Ishiwata K, Tajima H, et al. In vivo evaluation of [<sup>11</sup>C]SA4503 as a PET ligand for mapping CNS sigma1 receptors. *Nucl Med Biol.* 2000;27:255–261.
18. Kawamura K, Ishiwata K, Tajima H, et al. Preclinical evaluation of [<sup>11</sup>C]SA4503: radiation dosimetry, in vivo selectivity and PET imaging of sigma1 receptors in the cat brain. *Ann Nucl Med.* 2000;14:285–292.
19. Ishiwata K, Tsukada H, Kawamura K, et al. Mapping of CNS sigma1 receptors in the conscious monkey: preliminary PET study with [<sup>11</sup>C]SA4503. *Synapse.* 2001;40:235–237.
20. Ishii K, Ishiwata K, Kimura Y, Kawamura K, Oda K, Senda M. Mapping of sigma-1 receptors in living human brain [abstract]. *Neuroimage.* 2001;13:S984.
21. Kawamura K, Kimura Y, Tsukada H, et al. An increase of sigma receptors in the aged monkey brain. *Neurobiol Aging.* 2003;24:745–752.
22. Elsinga PH, Tsukada H, Harada N, et al. Evaluation of [<sup>18</sup>F]fluorinated sigma receptor ligands in the conscious monkey brain. *Synapse.* 2004;21:405–413.
23. Fujiwara T, Waterhouse RN, Yamamoto S, et al. Performance evaluation of a large axial field-of-view PET scanner: SET-2400W. *Ann Nucl Med.* 1997;11:307–313.
24. van Waarde A, Buursma AR, Kawamura K, Kobayashi T, Ishiwata K, Vaalburg W. Suitability of the sigma receptor ligand <sup>18</sup>F-FE-SA5845 for tumor imaging [abstract]. *J Nucl Med.* 2001;42(suppl):84P.
25. Seth P, Fei YJ, Li HW, Huang W, Leibach FH, Ganapathy V. Cloning and functional characterization of a sigma receptor from rat brain. *J Neurochem.* 1998;70:922–931.
26. Mei J, Pasternak GW. Molecular cloning and pharmacological characterization of the rat sigma1 receptor. *Biochem Pharmacol.* 2001;62:349–355.
27. Samoilova NN, Nagornaya LV, Vinogradov VA. (+)-[<sup>3</sup>H]SK&F 10,047 binding sites in rat liver. *Eur J Pharmacol.* 1988;147:259–264.
28. Roman F, Pascaud X, Chomette G, Bueno L, Junien JL. Autoradiographic localization of sigma opioid receptors in the gastrointestinal tract of the guinea pig. *Gastroenterology.* 1989;97:76–82.
29. Roman F, Pascaud X, Vauche D, Junien JL. Evidence for a non-opioid sigma binding site in the guinea-pig myenteric plexus. *Life Sci.* 1988;42:2217–2222.
30. Hellewell SB, Bruce A, Feinstein G, Orringer J, Williams W, Bowen WD. Rat liver and kidney contain high densities of sigma 1 and sigma 2 receptors: characterization by ligand binding and photoaffinity labeling. *Eur J Pharmacol.* 1994;268:9–18.
31. Liu Y, Whitlock BB, Pultz JA, Wolfe SA. Sigma-1 receptors modulate functional activity of rat splenocytes. *J Neuroimmunol.* 1995;59:143–154.
32. Paul R, Lavastre S, Floutard D, et al. Allosteric modulation of peripheral sigma binding sites by a new selective ligand: SR 31747. *J Neuroimmunol.* 1994;52:183–192.
33. van Waarde A, Cobben DCP, Suurmeijer AJH, et al. Selectivity of <sup>18</sup>F-FLT and <sup>18</sup>F-FDG for differentiating tumor from inflammation in a rodent model. *J Nucl Med.* 2004;45:695–700.

